Wind turbine simulation model for the study of combined mechanical and electrical faults

Raed Khalaf Ibrahim and Simon Watson
Centre for Renewable Energy Systems Technology (CREST),
School of Electronic, Electrical and Systems Engineering,
Loughborough University, UK
R.Ibrahim@lboro.ac.uk, S.J.Watson@lboro.ac.uk

***Abstract*—Wind turbine (WT) is a complex system comprised of many different components with different functions; it is a formidable challenge to understand the dynamic behaviour of a WT and the root cause of any disturbances, owing to the integration of aerodynamic, mechanical and electrical components in an environment subject to significant stochastic environment forcing. Therefore, there is a need for robust and reliable model to study the performance of WTs in terms of truly integrated electrical and mechanical responses. This paper presents a new model for WT by using MATLAB. This model can be simulated under various operating conditions to yield valuable information for condition monitoring and effective algorithm development for fault detection.**

***Index Terms*—Wind turbine, Combined simulation, MATLAB simulation, Fault detection.**

I. INTRODUCTION

Wind power is one of the world's fastest growing industries in recent years with countries striving to have more sustainable energy sources [1]. According to the global wind statistics of 2014, estimated by the global wind energy council (GWEC), wind power could reach 2,000 GW by 2030, and supply up to 17% -19% of global electricity by that time. By 2050, wind power could provide 25-30% of global electricity supply [2]. The European Wind Energy Association has envisioned that WT installations in the European Union will increase 64% by 2020 compared to 2013 levels [3]. Nevertheless, China foresees wind power capacity reaching 200 GW by 2020, 400 GW by 2030, and 1000 GW by 2050 [4].

As the large number of WTs are being installed and connected to power systems, it becomes more and more challenging for manufacturers to monitor and maintain WTs. Moreover, there is an additional cost might be caused, if WTs are not maintained timely. For example, failure of a $1500 bearing wind speeds could result in a $100,000 gearbox replacement, a $50,000 generator rewind and another $70,000 in expenses to replace the failed components [5]. This can be extremely expensive especially considering that onshore turbines are generally in isolated areas, such as mountains, deserts and offshore [6].

To make wind energy as an attractive alternative option of power generation, it is necessary to reduce maintenance costs and improve the reliability of WTs. Better designs of WT components is one of the most considerable solutions for this problem; the other is condition monitoring system of WTs [7]. Condition monitoring system is required to detect and diagnose WT failures in their early stages. This will lead to reduce maintenance cost, hardware damaging and unscheduled downtime. With these aims in mind, guaranteeing robust and reliable model for WT is required to provide enough data for reliable monitoring.

Many researchers have developed dynamic models for WTs with some level of accuracy [8][9]. However, it is a formidable challenge to understand the dynamic behaviour of a wind turbine and the root cause of any disturbances, owing to the integration of both mechanical and electrical components in an environment subject to significant stochastic environment forcing. Part of the problem is probably due to mechanical engineers are only focusing on mechanical properties without considering the transient stability of the power system such as faults, voltage and frequency dips and unbalanced voltages. Similarly, it is difficult for electrical engineers to consider mechanical events such as (damaging torque variations from the drivetrain, relationships between angular velocity and torque, the impact of the gear ratios, gear stages, etc.). These often separate electrical and mechanical approaches may lead to inaccurate and unrealistic models.

In this paper, the purpose of the work is to present a comprehensive model in order to enable studies involving the integration of aerodynamic, mechanical and electrical properties of a WT. With these aims, the possibility of using current signals which measured from the terminals of the generator can be used for fault studies. A signal processing algorithm based on Fast Fourier Transform (FFT) is applied to monitor the amplitude of fault frequencies.

II. WIND TURBINE MODELING

MATLAB is a very valuable tool in many different contexts. It makes it possible to investigate the expected general behavior and performance of a WT during the steady state or the transient stability. The MATLAB environment is really a cost-effective method to perform very thorough and detailed investigations before a prototype is exposed to real full-scale tests. Consequently, the time and development costs can be reduced considerably when the concept and detail design can be thoroughly tested without exposing the physical prototypes to the inuence of destructive full-scale tests. The turbine modeled in this paper is a variable speed wind turbine based on a multi-pole permanent magnet synchronous generator (PMSG). PMSG structure may or may not have a gearbox, and they are connected to the grid through a full-scale converter. But, using a gearbox would increase the speed of the generator shaft, and as a result, reduce the size of generator. The impact of the gearbox on the generator should, therefore, be investigated thoroughly in order to identify potential challenges and to develop measures to mitigate those issues. Accordingly, this work can provide an accurate and efficient way to analyze the interaction between mechanical system and electrical system in normal and fault operation. However, considering the modeling, WTs can be represented by a generic model as shown in Figure 1 [10].

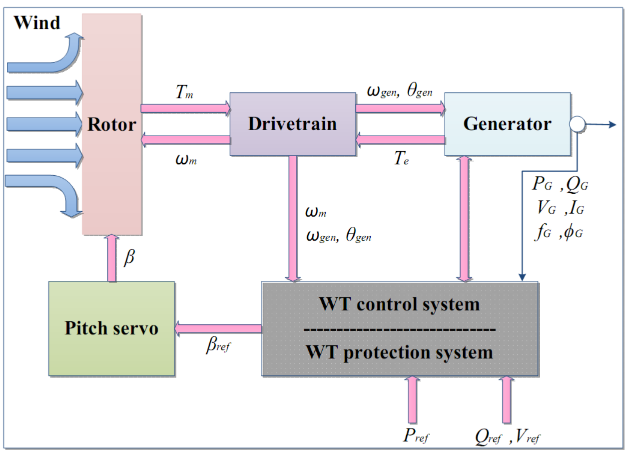

Fig. 1. Block diagram of a generic WT model. T_m: mechanical torque; ω_m: rotational speed of turbine; ω_{gen}: rotational speed of generator rotor; θ_{gen}: generator rotor angle; T_e: electrical torque; f_G: grid electrical frequency; ϕ_G: grid voltage phase angle; P_G: active power; Q_G: reactive power; V_G: grid voltage; I_G: grid current; P_{ref}: active power reference; Q_{ref}: reactive power reference; V_{ref}: grid voltage reference; β_{ref}: blade reference angle; β: pitch angle

The model consists of the following subsystems:

- Wind Speed Model;
- Rotor Model;
- Pitch Control System;
- Drivetrain Model;
- Generator model;
- Three-Phase RLC Load;

The schematic conguration used in this work is shown in Figure 2, and the important parameters used for this model are summarized in Table 1.

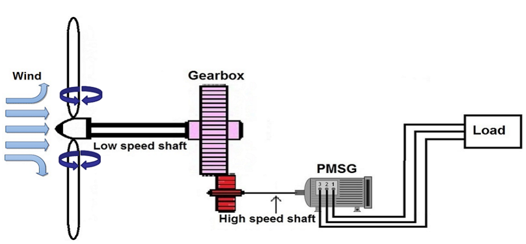

Fig. 2. Schematic diagram of the WT model

TABLE I
MODEL PARAMETERS.

Generator	
Line-Line Voltage (RMS)	400v
Frequency	50Hz
Stator phase resistance (ohm)	0.0018
Armature inductance (H)	0.000835
Inertia J(kg.m^2)	0.00062
Viscous damping F(N.m.s)	0.0003035
Pole pairs	2
Gearbox	
Gear Ratio	1: 70
Input speed (RPM)	21.4
Output speed (RPM)	1500

Some components are not considered in this paper, including yaw systems, tower, bearings, brakes model and power converter. This is not considered a problem, because the main topic of interest in this work is to combine the aerodynamic, mechanical and electrical components in normal and fault operation, and the impact of those components on the stator current can be assumed to be rather limited. The subsystem models of WT are presented below.

A. Wind Speed Model

This model is used to generate a short-term wind speed variations with certain characteristics, such as speed range or turbulence intensity, which a WT will experience. The wind speed v_w is modeled as the sum of the four components [11].

$$v_w(t) = v_{avg} + v_r(t) + v_g(t) + v_n(t) \tag{1}$$

where v_{avg} is the average value of the wind speed, $v_r(t)$ is the ramp wind component, $v_g(t)$ is the gust wind component and $v_n(t)$ is the base noise wind component, all of them in m/s. Figure 3 shows the graphics of the non-constant wind speed components: average, ramp, gust and noise components.

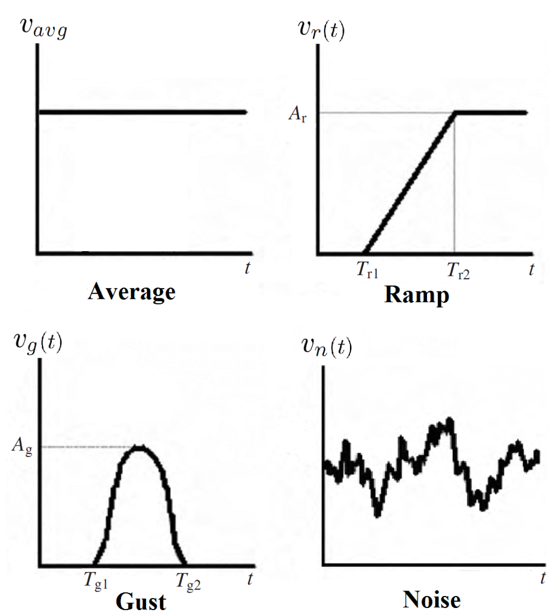

Fig. 3. wind speed components

An example of a wind speed sequence generated using this approach is shown in Figure 4. The parameters used were v_{avg}= 12, Tg = 90, Tg =250, Ag = 1.5, Ar = 2, Tr = 400, Tr= 500.

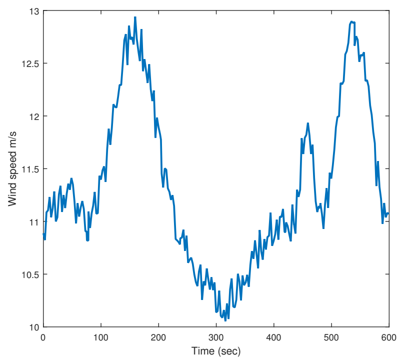

Fig. 4. Example of a simulated wind speed sequence

B. Rotor Model

The rotor transfers the kinetic energy from the wind into mechanical energy at the rotor shaft by aerodynamic forces producing lift on the blades. The kinetic energy of a cylinder of air of radius R traveling with wind speed v_w corresponds to a total wind power P_w within the rotor swept area of WT. This power, P_w, can be expressed by

$$P_w = \frac{1}{2}\rho\pi R^2 v_w^3 \tag{2}$$

where ρ is the air density (1.225 kg/m3), R is the rotor radius and V_{wind} is the wind speed. It is important to note that the rotor blades are designed to extract a maximum power from the wind, but it is not possible to convert all the air kinetic energy into electrical energy since the air would stand behind the turbine and it reduces the resulting wind speed. In other words, the wind speed is only reduced by the rotor blades, which thus extract a fraction of the power in the wind. This fraction is denominated the power efficiency coefficient C_P of the WT. The mechanical power P_m of the WT is therefore, by the definition of C_P, given by the total power in the wind P_{wind} using the following equation:

$$P_m = C_P P_w \tag{3}$$

A WT has a maximum level of power which can be extracted from the wind so that the theoretical maximum energy that can be extracted is with C_P = 0.599 and is termed the Betz limit. In practice the coefficient of performance is less than this and also depends on the specific WT shape, the wind velocity, the turbine rotor speed, and the turbines blade pitch, where the general function defining C_P as a function of the tip-speed ratio λ and the blade pitch angle β is defined as [12]

$$C_P(\lambda, \beta) = c_1(\frac{c_2}{\lambda_i} - c_3\beta - c_4\beta^{c_5} - c_6)\exp(-\frac{c_7}{\lambda_i}) \tag{4}$$

where

$$\lambda_i = [(\frac{1}{\lambda + C_8\beta}) - (\frac{c_9}{\beta^3 + 1})]^{-1} \tag{5}$$

Equations (4) and (5) are used to calculate the impact of the pitch angle on the power coefcient. The resulting value can be inserted into Equation (2) to calculate the mechanical power extracted from the wind. The values of the constants can be found in [12].

If the mechanical torque T_m is to be applied instead of the mechanical power P_m, it can be easily calculated from the dynamic theory of rotating devices in physics by using the turbine rotational speed ω_m:

$$T_m = \frac{P_m}{\omega_m} \tag{6}$$

where

$$\omega_m = \frac{\lambda v_w}{R} \tag{7}$$

Equations (2) and (6) are very important equations which combine the concepts of mechanical power, mechanical torque and total wind power.

C. Pitch Control System

The pitch control system is active only in high wind speeds above 12m/s. In these circumstances, the rotor speed can no longer be controlled by increasing the generated power, as this would lead to overloading the generator. Thus, the blade pitch angle is changed in order to limit the aerodynamic efficiency of the rotor. This prevents the rotor speed from becoming too high, which would result in mechanical damage. The flow chart shown in Figure 5 shows the different steps to calculate the pitch angle.

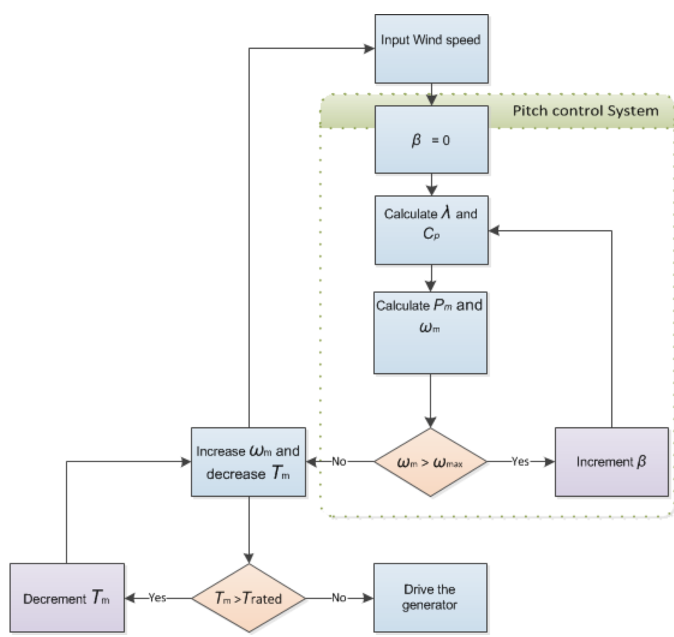

Fig. 5. Flow chart of the pitch control system

The optimal pitch angle is zero below the nominal wind speed. From the nominal wind speed onwards, the optimal angle increases steadily with increasing wind speed. The performance of the model has been investigated under variable speed conditions in order to verify the performance of the pitch model. Figure 6 shows short-term wind speed variations of interest as input wind speed to the model. So, the mechanical power extracted from the wind is shown in Figure 7. It is clear that when the wind speed increases, the mechanical power increases until the pitching starts, when the speed reaches the rated speed, 12m/s. While the blades pitch, the mechanical torque decreases.

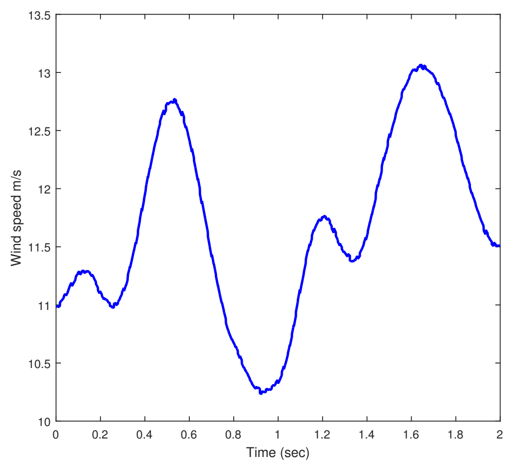

Fig. 6. Wind speed input to the model

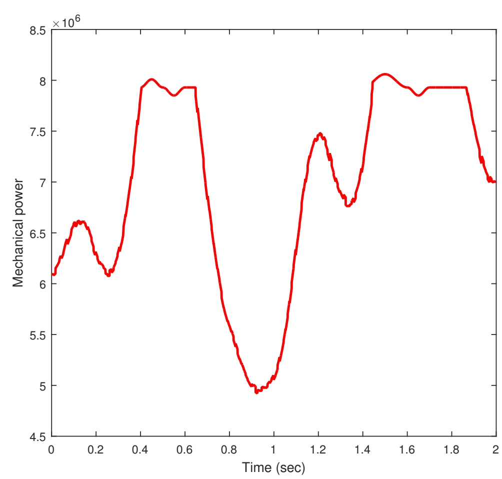

Fig. 7. The power extracted from the wind

D. Drivetrain Model

The drive train consists of the following elements: a low speed shaft, a gearbox and a high speed shaft. The model outputs of the transmitted torque T_l ,through the shaft regarding the speed difference between the driving side and the loaded side of the shaft, is given by the following equation [13]:

$$T_l = K \int (\omega_d - \omega_l) + B(\omega_d - \omega_l)dt \tag{8}$$

where K (N.m.) is the shaft stiffness, B (N.m.s.) is the internal damping, and ω_d, ω_l are the speeds (rad/s) of the driving side and the loaded side, respectively. While the mathematical model of the gearbox is described with the following equations:

$$\begin{aligned} \omega_1 &= N\omega_2 \\ T_2 &= NT_1 \\ P_1 &= \omega_1 T_1 \\ P_2 &= -\omega_2 T_2 \end{aligned} \tag{9}$$

where ω_1 is input shaft angular velocity, ω_2 is the output shaft angular velocity, N is the gear ratio, T_1 is the torque on the input shaft, T_2 is the torque on the output shaft, and P_1, P_2 are the power on the input shaft and the output shaft, respectively.

E. Generator model

Most modern large-scale variable speed WTs are based on doubly-fed induction generator (DFIG) and permanent magnet synchronous generator (PMSG). Therefore, PMSG is studied in this work. It must be noted that PMSG structure may or may not have a gearbox, and they are connected to the grid through a full-scale converter. But, using a gearbox would increase the speed of the generator shaft, and as a result, reduce the size of generator. However, the detail description and model equation derivation of PMSG can be found in most power system and electric machine references. The PMSG model can be described using following equations in the d-q rotor reference frame:

$$\frac{\partial}{\partial t} i_{ds} = \frac{1}{L_d} v_{ds} - \frac{R_s}{L_d} i_{ds} + \frac{L_q}{L_d} \omega_r i_{qs} \tag{10}$$

$$\frac{\partial}{\partial t} i_{qs} = \frac{1}{L_q} v_{qs} - \frac{R_s}{L_q} i_{qs} - \frac{L_d}{L_q} \omega_r i_{ds} - \frac{\omega_r}{L_q} \psi_m \tag{11}$$

$$T_e = 1.5 n_p [\psi_m i_{qs} + (L_d - L_q) i_{ds} i_{qs}] \tag{12}$$

$$\frac{\partial}{\partial t} \omega_r = \frac{n_p}{J} (T_e - T_m) \tag{13}$$

$$\frac{\partial}{\partial t} \theta_r = \omega_r \tag{14}$$

where d and q refer to the physical quantities that have been transformed into the d-q synchronous rotating reference frame, i_{ds} and i_{qs} are the stator currents on the d and q axis, respectively. R_s is the stator resistance, ψ_m is the permanent magnetic flux and n_p is the pole pairs , ω_r, θ_r and J are the angular velocity of the rotor, the rotor angular and inertia of rotor, respectively.

III. SIMULATION RESULTS

In this section, the electrical responses to the generated wind speed are presented. The wind speed input used in these simulations is that shown in Figure 6, and the mechanical power extracted from the wind is shown in Figure 7. The WT rotor drives the generator through the gearbox that steps up the drive train rotational speed from about 20 rpm at the low-speed shaft to 1500 rpm at the high-speed shaft. As mentioned before, the model described enables studies involving the integration of aerodynamic, mechanical and electrical properties of a WT drive train. The model allows the study of the impact of high-ramping wind speed events on the power system, as well as the impact of turbulence on the voltage and frequency, and this can be seen on the electromagnetic torque and the stator currents of the generator in Figure 8 and Figure 9, respectively.

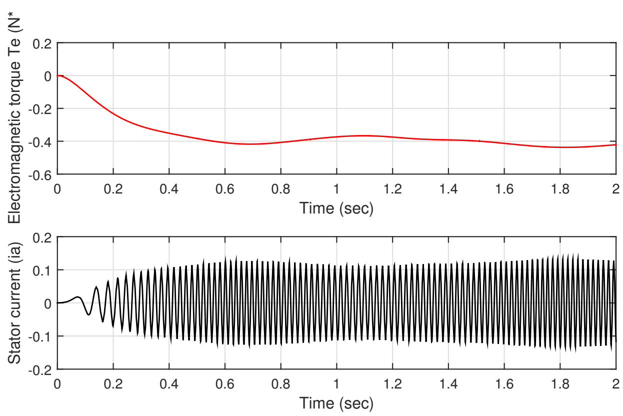

Fig. 8. PMSG electromagnetic torque and the stator current (i_a)

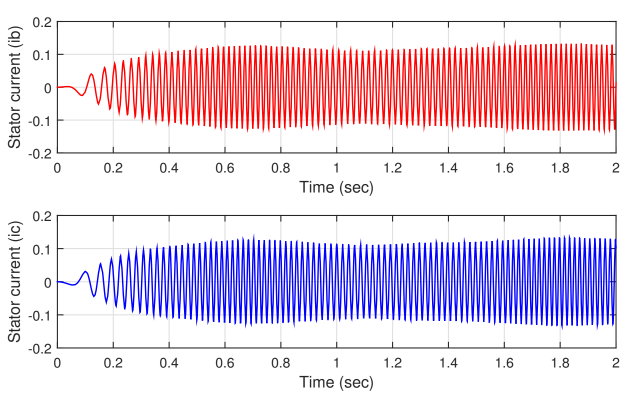

Fig. 9. PMSG stator currents (i_b) and (i_c)

The simulation results of the generator response show that the speed, however, contains an oscillatory component, which is reected in the generator output, particularly the electromagnetic torque and the stator currents. Without any electrical control, the mechanical oscillations can be seen at the output. Furthermore, the model is capable to simulate the transient responses of WT during different faults. For example, to verify the possibility to recognize useful features in generator signals when a mechanical fault occurs, a fault has been simulated by applying a friction force to change the low speed shaft during a simulation. The harmonic spectra of the healthy and faulty system was obtained bu applying the fast furrier transform (FFT) algorithm to the stator current as shown in Figure 10.

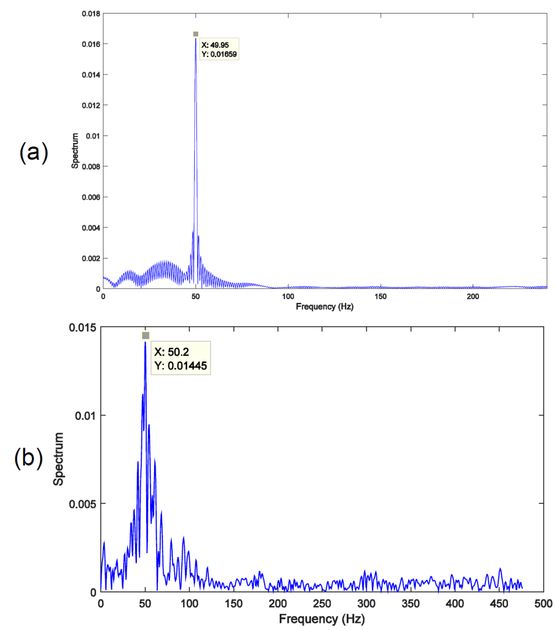

Fig. 10. (a) Power spectrum of healthy WT. (b) Power spectrum of faulty WT.

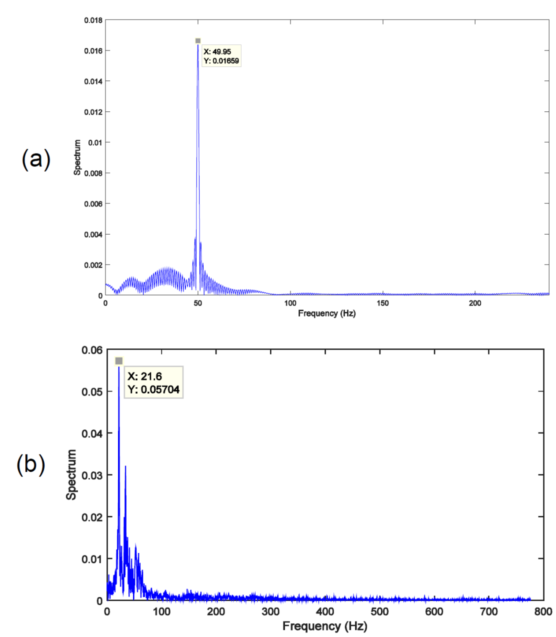

Fig. 11. (a) Power spectrum of healthy WT. (b) Power spectrum of faulty WT.

In the this work, another case study presented short circuits in the stator windings to ground which has been applied to see the characteristic and the shape of the stator current during the fault. Figure 11 shows that the stator winding fault can be well identified using the FFT algorithm. Compared to the previous case study, stronger oscillations of the current signal can be observed.

IV. Conclusion

In this work, a WT model is built in the MATLAB/Simulink environment. The model can simulate various operating conditions to study a WT in terms of its integrated aerodynamic, mechanical and electrical performance. The possibility of using current signals measured from the terminals of the generator is also investigated, and an FFT is applied to detect fault frequencies. The simulation results have shown that frequency components related to faults can be clearly recognized in the current spectrum. This model shows promising results and should provide an appropriate theoretical test bed for WT condition monitoring and effective algorithm development for fault detection, though further work is needed to model the different components of the WT in sufficient detail.

References

[1] J.-h. Shin, Y.-S. Lee, and J.-O. Kim, "Fault prediction of wind turbine by using the svm method," in *Information Science, Electronics and Electrical Engineering (ISEEE), 2014 International Conference on*, vol. 3, pp. 1923–1926, IEEE, 2014.

[2] F. Lauha, S. Steve, S. Sgruti, and Q. Limig, "Global wind report annual market update 2013," *Global Wind Energy Council*, 2012.

[3] "Wind energy scenarios for 2020." The European Wind Energy Association, 2014.

[4] "China wind energy development roadmap 2050." International Energy Agency (IEA), Energy Research Institute (ERI) and National Development and Reform Commission (NDRC) of P. R. China, 2011.

[5] R. Hyers, J. McGowan, K. Sullivan, J. Manwell, and B. Syrett, "Condition monitoring and prognosis of utility scale wind turbines," *Energy Materials*, vol. 1, no. 3, pp. 187–203, 2006.

[6] P. J. Tavner, D. Zappal, S. Sheng, and C. J. Crabtree, "Side-band algorithm for automatic wind turbine gearbox fault detection and diagnosis," *IET Renewable Power Generation*, vol. 8, pp. 380–389, May 2014.

[7] M. Wilkinson, B. Darnell, T. van Delft, and K. Harman, "Comparison of methods for wind turbine condition monitoring with scada data," *IET Renewable Power Generation*, vol. 8, no. 4, pp. 390–397, 2014.

[8] W. Yingying, L. Qing, and Q. Shiyao, "A new method of wind turbines modeling based on combined simulation," in *Power System Technology (POWERCON), 2014 International Conference on*, pp. 2557–2563, IEEE, 2014.

[9] M. Yin, G. Li, M. Zhou, and C. Zhao, "Modeling of the wind turbine with a permanent magnet synchronous generator for integration," in *Power Engineering Society General Meeting, 2007. IEEE*, pp. 1–6, IEEE, 2007.

[10] D. Ochs, R. Miller, and W. White, "Simulation of electromechanical interactions of permanent-magnet direct-drive wind turbines using the fast aeroelastic simulator," *Sustainable Energy, IEEE Transactions on*, vol. 5, pp. 2–9, Jan 2014.

[11] P. Anderson and A. Bose, "Stability simulation of wind turbine systems," *Power Apparatus and Systems, IEEE transactions on*, no. 12, pp. 3791–3795, 1983.

[12] S. Heier, *Grid integration of wind energy conversion systems*. 2nd edition, John Wiley Sons, Inc, 2006.

[13] R. L. Norton, *Machine Design*. Prentice Hall, 1998.